

Inhibition of FcεRI-mediated mast cell responses by ES-62, a product of parasitic filarial nematodes

Alirio J Melendez¹, Margaret M Harnett², Peter N Pushparaj¹, WS Fred Wong³, Hwee Kee Tay¹, Charles P McSharry² & William Harnett⁴

Atopic allergy is characterized by an increase in IgE antibodies that signal through the high-affinity Fcε receptor (FcεRI) to induce the release of inflammatory mediators from mast cells. For unknown reasons, the prevalence of allergic diseases has recently increased steeply in the developed world¹. However, this increase has not been mirrored in developing countries², even though IgE concentrations are often greatly elevated in individuals from these countries, owing to nonspecific IgE induction by universally present parasitic worms³. Here we offer one explanation for this paradox based on the properties of ES-62, a molecule secreted by filarial nematodes⁴. We found that highly purified, endotoxin-free ES-62 directly inhibits the FcεRI-induced release of allergy mediators from human mast cells by selectively blocking key signal transduction events, including phospholipase D-coupled, sphingosine kinase-mediated calcium mobilization and nuclear factor-κB activation. ES-62 mediates these effects by forming a complex with Toll-like receptor 4, which results in the sequestration of protein kinase C-α (PKC-α). This causes caveolae/lipid raft-mediated, proteasome-independent degradation of PKC-α, a molecule important for the coupling of FcεRI to phospholipase D and mast cell activation. We also show that ES-62 is able to protect mice from mast cell-dependent hypersensitivity in the skin and lungs, indicating that it has potential as a novel therapeutic for allergy.

ES-62 is a glycoprotein secreted by filarial nematodes—important parasites of humans—that is anti-inflammatory largely by virtue of covalently attached phosphorylcholine moieties⁴. The full extent of ES-62's interactions with the immune system of the parasitized host is unknown, but we hypothesized that it might interact directly with, and therefore inhibit the function of, mast cells. Cross-linking of FcεRI triggers mast cell activation, leading to exocytosis of granules containing preformed inflammatory mediators and to *de novo* synthesis of pharmacologically active eicosanoids and proinflammatory cytokines⁵. We thus pretreated human mast cells with ES-62 at a concentration that was within the range found for phosphorylcholine-containing products in the bloodstreams of filaria-infected humans⁶ to determine

whether degranulation could be inhibited (Fig. 1). We found that preincubation with ES-62 indeed inhibited FcεRI-triggered release of β-hexosaminidase, a marker of mast cell degranulation (Fig. 1a). This inhibition did not reflect downmodulation of FcεRI expression on the cell surface (Supplementary Fig. 1 online). Moreover, the FcεRI-mediated tyrosine phosphorylation of target proteins required for the recruitment of signals essential for mast cell degranulation, such as calcium mobilization and protein kinase C (PKC) activation⁵, was not affected in ES-62-treated cells (Supplementary Fig. 1). These data indicate that ES-62 does not act by affecting FcεRI expression or the early tyrosine kinase-dependent events after its cross-linking. Consistent with this, ES-62 pretreatment also inhibits the β-hexosaminidase release triggered by phorbol myristate acetate (Supplementary Fig. 1), which by directly activating PKC, bypasses receptor activation.

Instead, we found that ES-62 inhibited the initial peak of Ca²⁺ mobilization triggered by FcεRI, but not the delayed, more sustained response (Fig. 1b). We have previously shown that the former is elicited by the sequential activation of phospholipase D (PLD) and sphingosine kinase (SPHK), whereas sustained entry of Ca²⁺ is dependent on the activation of phospholipase C (PLC), which generates inositol trisphosphate from phosphatidylinositol-4,5-bisphosphate⁷. Consistent with this, pretreatment of cells with ES-62 inhibits FcεRI-coupled PLD (Fig. 1c) and SPHK (Fig. 1d) activities, whereas PLC-γ1 translocation (Supplementary Fig. 1) and inositol trisphosphate generation (Supplementary Fig. 1) proceed as normal. Our earlier work demonstrated that PKC-α expression is essential for FcγRI coupling to PLD in monocytes⁸, and exposure of mast cells to ES-62 leads to downregulation of several PKC isoforms, with PKC-α being the most strongly affected isoform (Fig. 1e). By using antisense knockdown^{7,8} to reduce PKC-α levels by ~80% (Supplementary Fig. 1), we now show that PKC-α expression is not only required for FcεRI-coupling to PLD (Fig. 1f), but also for degranulation in mast cells (Fig. 1g). This result is consistent with reports that PKC-α is an important regulator of FcεRI-mediated mast-cell responses^{9,10}. Collectively, our findings indicate that downregulation of PKC-α provides a mechanism for ES-62-mediated inhibition of PLD and the consequent calcium mobilization.

¹Department of Physiology, Yong Loo Lin School of Medicine, National University of Singapore, 2 Medical Drive MD9, Singapore 117597. ²Division of Immunology, Infection and Inflammation, Glasgow University, 120 University Place, Glasgow G12 8TA, UK. ³Department of Pharmacology, Yong Loo Lin School of Medicine, National University of Singapore, 2 Medical Drive MD2, Singapore 117597. ⁴Strathclyde Institute of Pharmacy and Biomedical Sciences, Strathclyde University, 27 Taylor Street, Glasgow G4 0NR, UK. Correspondence should be addressed to W.H. (w.harnett@strath.ac.uk).

Received 5 January; accepted 21 August; published online 21 October 2007; doi:10.1038/nm1654

Pharmacologically active leukotrienes and prostaglandins are synthesized from the arachidonic acid released by the breakdown of membrane phospholipids by cytosolic phospholipase A₂ (PLA₂) during mast-cell degranulation⁵. As ES-62 inhibits degranulation and prevents the increase in cytoplasmic Ca²⁺ that is necessary for activation of PLA₂, we expected it to block the production of such mediators, and we indeed observed this (Fig. 2a,b and Supplementary Fig. 2 online). Prostaglandin D₂ (PGD₂) and leukotriene C₄ (LTC₄), both of which were targeted, are particularly important lipid-derived mediators with respect to mast-cell activities. Mast-cell activation also results in sustained *de novo* production of a number of cytokines that may contribute to the pathology underlying allergic disease^{5,11,12}. Pre-exposure to ES-62 substantially inhibited FcεRI-triggered generation of tumor necrosis factor-α (TNF-α; Fig. 2c) and interleukin (IL)-6 and IL-3 (Supplementary Fig. 2), but not IL-13 (Fig. 2d) or IL-5 (Supplementary Fig. 2). This indicates that

ES-62 can inhibit proinflammatory, but not certain type 2 helper T cell (T_H2; IL-4 was not detected), cytokine production by human mast cells.

Notably, whereas proinflammatory cytokine production is dependent on nuclear factor (NF)-κB (p50 and p65 subunits) signaling in mast cells^{11,13}, the induction of T_H2-like cytokines has recently been reported to be NF-κB independent^{12,14}, and hence we investigated the effect of ES-62 on the activation of this transcription factor. FcεRI-triggered activation of both NF-κB p50 and p65 was abrogated in cells pretreated with ES-62 (Fig. 2e). Of note, roles in NF-κB activation have been shown for both Ca²⁺ signal amplitude and frequency and PKC isoforms such as PKC-α, PKC-β, PKC-δ, PKC-ι and PKC-ζ (refs. 5,9,10,13–15), the expression of all of which is reduced in ES-62-treated cells (Fig. 1e). Consistent with the decrease in expression of these NF-κB-targeting PKC isoforms, we found a substantial decrease in FcεRI-stimulated total PKC activity in ES-62-treated cells (Fig. 1h).

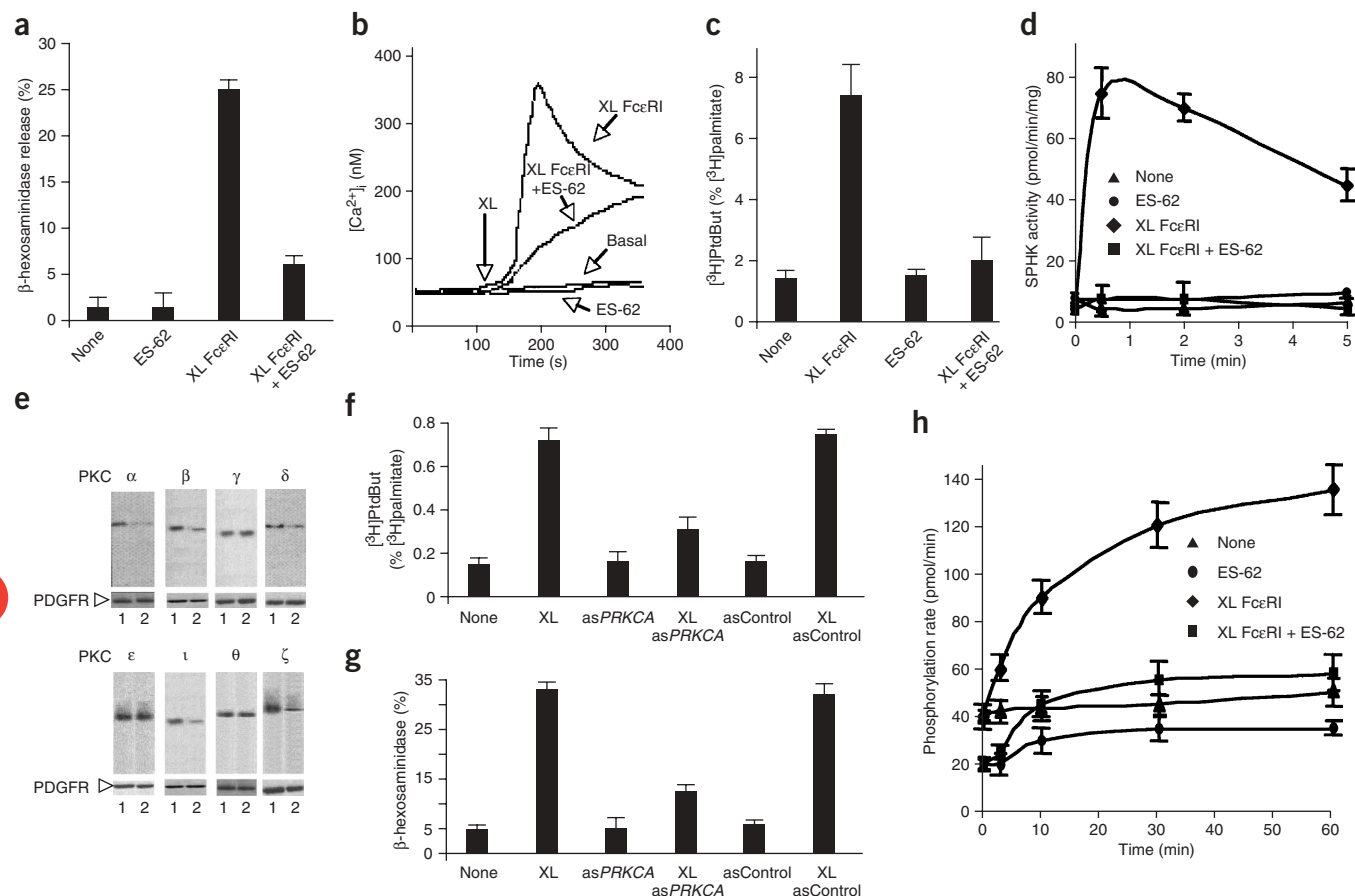


Figure 1 ES-62 inhibition of FcεRI-mediated Ca²⁺ mobilization and degranulation of human BMMC correlates with downregulation of PKC-α expression. (a–d) β-hexosaminidase release (a), calcium mobilization (b), PLD activity (c) and SPHK activity (d) were determined after crosslinking of IgE antibodies bound to FcεRI (XL FcεRI) by addition of DNP-HSA for 30 min (a,c) or the times indicated (b,d) in control and ES-62-treated cells⁷. Results shown are means ± s.d., *n* = 3. PtdBut, phosphatidylbutanol. (e) Extracts from control BMMCs (lane 1) or from cells pretreated overnight with ES-62 (lane 2) were analyzed for PKC-α, PKC-β, PKC-γ, PKC-δ, PKC-ε, PKC-ι, PKC-θ and PKC-ζ expression. Blots were also probed with antibody to platelet-derived growth factor receptor (PDGFR) to confirm equal loading. Quantitative densitometric analysis revealed the following levels of PKC expression in ES-62-treated cells, expressed as percentages of PKC expression levels in matched, untreated cells: PKC-α, 15% ± 10%, *n* = 3; PKC-β, 32% ± 18%, *n* = 3; PKC-γ, 120% ± 25%, *n* = 5; PKC-δ, 44% ± 14%, *n* = 5; PKC-ε, 95% ± 27%, *n* = 5; PKC-ι, 35% ± 23%, *n* = 3; PKC-θ, 100% ± 10%, *n* = 3; and PKC-ζ, 30% ± 13%, *n* = 3. Results are expressed as means ± s.d., with *n* = number of experiments. (f–h) PLD activity (f), β-hexosaminidase release (g) and PKC activity (h) were determined after crosslinking of IgE antibodies bound to FcεRI by addition of DNP-HSA for 30 min (f,g) or the times indicated (h) in control and ES-62-treated cells⁷. In f and g, cells were incubated with or without 10 μM phosphorothioate-protected antisense oligonucleotides (asPRKCA, specific for PKC-α; asControl, scrambled control oligonucleotide) for 48 h before FcεRI crosslinking. All data are representative of at least three separate experiments. Results shown are means ± s.d., *n* = 3. XL indicates crosslinking.

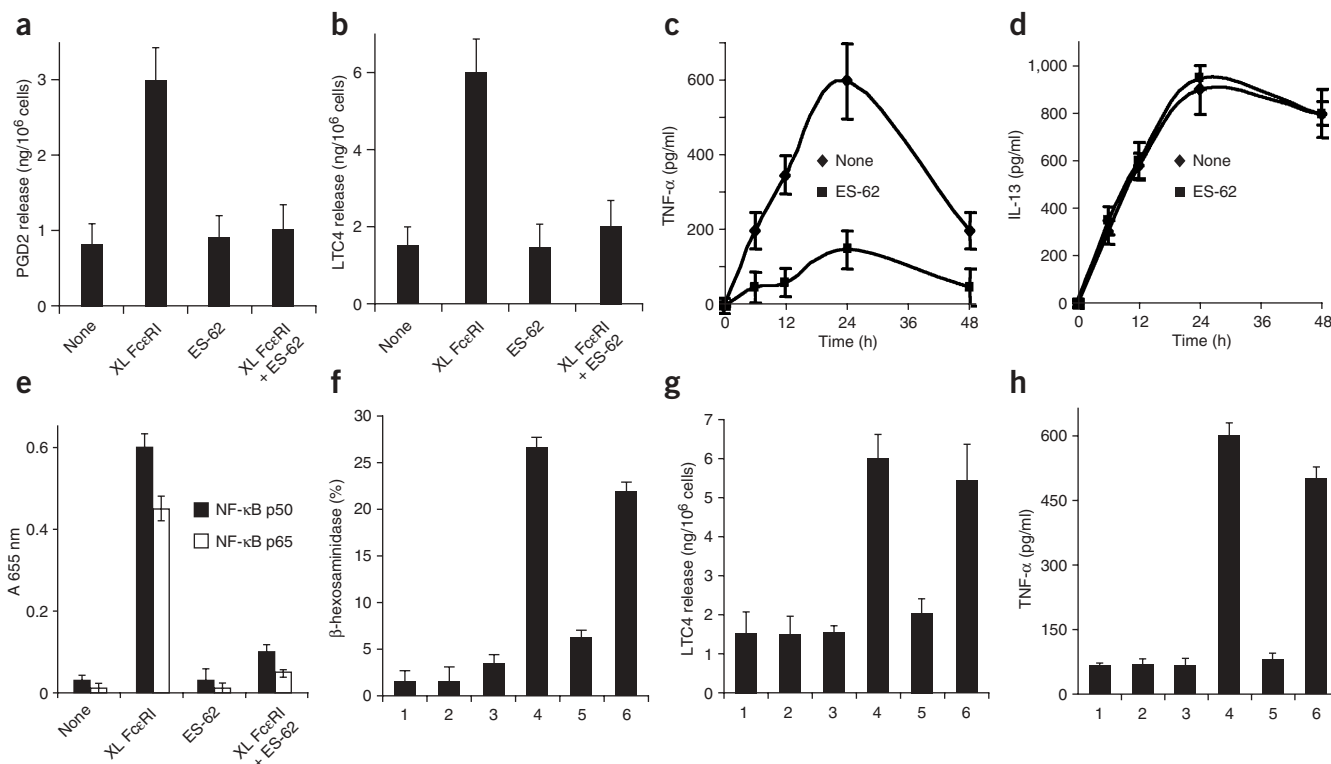


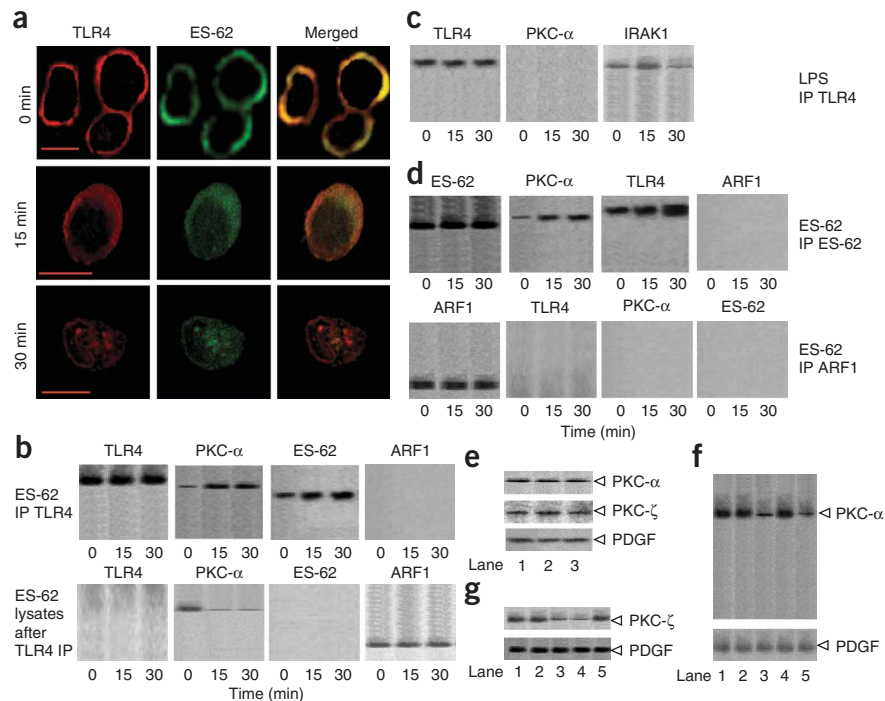
Figure 2 ES-62-mediated inhibition of proinflammatory mediator production from BMMCs correlates with decreased NF-κB activity, and TLR4 antisense oligonucleotides prevent ES-62 modulation of mast cell function. **(a–d)** PGD2 **(a)**, LTC4 **(b)**, TNF-α **(c)** and IL-13 **(d)** release was determined after cross-linking of IgE bound to FcεRI by DNP-HSA for 24 h, or the times indicated, in control and ES-62-treated cells. Results are expressed as means ± s.d. Analysis of pooled data from three experiments revealed substantial reductions in ES-62-treated samples after subtraction of basal level values: PGD2, 85% ± 10%; LTC4, 87% ± 10%; TNF-α (24 h), 75% ± 15%. **(e)** Nuclear extracts from FcεRI-stimulated BMMCs were probed for NF-κB p50 or p65 binding activity. Reduction of NF-κB activity induced by ES-62 is 87% ± 5 for p50 and 90% ± 5 for p65 (means ± s.d. from three separate experiments). **(f–h)** BMMCs were incubated in the absence (lanes 1, 2, 4 and 5) or presence (lanes 3 and 6) of a TLR4 antisense oligonucleotide for 48 h. After 30 h, ES-62 (lanes 2, 3, 5 and 6) and DNP-specific IgE antibodies (lanes 4–6) were added. After crosslinking of FcεRI, β-hexosaminidase release was determined at 30 min **(f)**, and LTC4 **(g)** and TNF-α **(h)** release were measured at 24 h. Results shown are means ± s.d., *n* = 3. Analysis of pooled data from three experiments, normalized to control FcεRI responses (defined as 100%) after subtraction of basal values, revealed that FcεRI-triggered cells pretreated with ES-62 showed 18 ± 5% degranulation, 11 ± 7% LTC4 release and 3 ± 2% TNF-α release, whereas cells pretreated with ES-62 and asTLR4 showed 78 ± 10% degranulation, 75 ± 10% LTC4 release and 81 ± 10% TNF-α release.

We have previously shown in knockout mice that ES-62-mediated modulation of macrophage proinflammatory cytokine production depends on Toll-like receptor 4 (TLR4)¹⁶. Compared to signaling induced by lipopolysaccharide (LPS), the classical TLR4 ligand, ES-62-mediated TLR4 signaling has unusual features: in particular, ES-62-mediated signaling does not require TLR4 Pro712, which is crucial for LPS signaling¹⁷. However, the mechanism of subversion of TLR4 signaling by ES-62 has not previously been delineated. Here we show that antisense reduction of TLR4 expression in mast cells (by 80%; **Supplementary Fig. 3** online) prevented ES-62-mediated inhibition of degranulation (**Fig. 2f**) and the consequent release of eicosanoids and proinflammatory cytokines (**Fig. 2g,h** and **Supplementary Fig. 3**). To investigate whether ES-62 was employing TLR4 as a receptor, we assessed the localization of both molecules in mast cells by confocal microscopy (**Fig. 3a**). We incubated mast cells with FITC-conjugated ES-62 and examined its colocalization with TLR4 at various timepoints. At time 0, the molecules colocalized at the cell surface, but thereafter, substantial proportions of both were internalized. Again, colocalization was apparent; the punctate staining suggested that ES-62–TLR4 complexes were being trafficked into vesicular compartments within 15 min. Moreover, there was evidence

of perinuclear localization of the ES-62–TLR4 complexes, with some expression also detected within the nucleus after 30 min of incubation (**Fig. 3a**).

We next investigated whether this trafficking of ES-62–TLR4 complexes drove ES-62-mediated downregulation of PKC-α expression. Analysis of the composition of TLR4-containing immune complexes by western blotting (**Fig. 3b**) revealed the presence of ES-62 in these complexes. At time 0, low levels of PKC-α were also present, but within 15 min, by which point the ES-62–TLR4 complexes appeared to have entered the vesicular compartment, the amount of bound PKC-α was found to have increased greatly (**Fig. 3b**). As a negative control, the blots were also probed for ADP-ribosylation factor-1 (ARF1), and we found this signaling element to be absent. Furthermore, analysis of the TLR4-depleted lysates demonstrated that all the ES-62 had been depleted from the time 0 lysate (**Fig. 3b**), a result consistent with its association with TLR4 at the plasma membrane. In contrast, PKC-α was depleted with kinetics that corresponded to its association with ES-62–TLR4. These results suggest that ES-62–TLR4 complexes may sequester PKC-α from FcεRI and PLD at the plasma membrane¹⁸, and the subsequent internalization of ES-62–TLR4 complexes may drive trafficking of PKC-α to the perinuclear region,

Figure 3 ES-62 forms a complex with TLR4 and PKC- α and is internalized into vesicular compartments. **(a,b)** BMMCs were incubated with FITC-conjugated ES-62 at 4 °C for 30 min, washed and incubated at 37 °C for the times specified and then analyzed for TLR4 and ES-62 expression with a Zeiss LSM510 confocal microscope (**a**; scale bar equals 25 μ m) or subjected to digitonin lysis (**b**). For **b**, cell lysates (50 μ g) were immunoprecipitated with antibody to TLR4 (IP TLR4) and probed for TLR4, ES-62–FITC, PKC- α and ARF1 by western blotting with the appropriate antibodies. In **b**, samples of the remaining lysates (150 μ g) were also probed with the antisera. **(c)** Cells were incubated with LPS (500 ng/ml) for 30 min at 37 °C and cell lysates were prepared as above. The lysates were immunoprecipitated with antibody to TLR4 and probed for TLR4, PKC- α and IRAK1. **(d)** Cells were prepared and subjected to digitonin lysis as in **b** above. Cell lysates were immunoprecipitated with antibody to FITC (IP ES-62) or ARF1 (IP ARF1) and probed for TLR4, ES-62–FITC, PKC- α and ARF1 by western blotting with the appropriate antibodies. **(e)** BMMCs were incubated with vehicle (lane 1), nystatin (50 μ g/ml; lane 2) or lactacystin (25 μ M; lane 3) overnight at 37 °C and then cell lysates were probed by western blotting for PKC- α , PKC- ζ and PDGF (loading control). **(f,g)** BMMCs were incubated with vehicle (lanes 1–3), nystatin (50 μ g/ml; lane 4) or lactacystin (25 μ M; lane 5) for 30 min before culture overnight with media (lane 1), LPS (lane 2) or ES-62 (lanes 3, 4 and 5). Cell lysates were prepared and probed by blotting as in **e**; PKC- α blotting is shown in **f** and PKC- ζ blotting is shown in **g**, each with the PDGF control.



where it can be targeted for degradation¹⁹. Notably, we also observed that PKC- α was not sequestered by TLR4 when the cells were exposed to LPS (**Fig. 3c**), again highlighting that the consequences of interactions between TLR4 and the bacterial product are different from those between TLR4 and ES-62. LPS was active in this experiment as it triggered interleukin-1 receptor–associated kinase-1 association with the TLR4 signaling scaffold with the expected kinetics²⁰. Further support for the ES-62–TLR4–PKC- α association was provided by parallel ES-62 pull-down studies, which showed that such ES-62–containing immune complexes contained TLR4 and an amount of PKC- α that increased with time, but did not contain ARF1 (**Fig. 3d**). In contrast, ARF1-containing immune complexes lacked TLR4, ES-62 and PKC- α at all time points (**Fig. 3d**). It is possible that other PKC isoforms targeted by ES-62 (**Fig. 1e**) are also sequestered in a TLR4-dependent manner, and this may further contribute, through reduced NF- κ B activation, to suppressed mast cell function. Nevertheless, PKC- α is critical for PLD activation and mast cell degranulation (**Fig. 1f,g**). Thus, overall, the sequestration and degradation of PKC- α by ES-62–TLR4 complexes provides a mechanism for the disruption of key PLD–SPHK–dependent pathways of calcium, PKC and NF- κ B activation; the disruption of these pathways is associated with the consequent failure of ES-62–treated mast cells to degranulate in response to cross-linking of Fc ϵ RI.

Studies in IEC-18 rat intestinal epithelial cells revealed that PKC- α can be degraded by two distinct mechanisms: a ubiquitin–proteasome–dependent pathway or caveolae/lipid raft–mediated trafficking to a perinuclear location followed by proteasome-independent degradation¹⁹. Our confocal microscopy data (**Fig. 3a**) suggest that ES-62 uses the latter pathway. To investigate this, we determined the effects of lactacystin and nystatin, inhibitors of the proteasomal and the caveolae/lipid raft–mediated pathways, respectively¹⁹, on ES-62–mediated downregulation of PKC- α expression. After establishing

that, as in IEC-18 cells¹⁹, neither reagent had any effect on PKC- α expression when added to mast cells (**Fig. 3e**), we found that whereas nystatin blocked ES-62–mediated downregulation of PKC- α , lactacystin had no effect (**Fig. 3f**). Lactacystin was shown to be active, as it was able to protect another ES-62 target, PKC- ζ (**Fig. 3g**), which has previously been reported to be degraded in a ubiquitin–proteasome–dependent manner²¹. Nystatin was ineffective against PKC- ζ , confirming that this PKC target of ES-62 was not degraded by the caveolae/lipid raft–mediated pathway and thereby revealing a difference between the mechanisms of degradation of the two PKC isoforms. Moreover, we also found that, in contrast to ES-62–mediated TLR4 signaling, LPS-mediated TLR4 signaling does not downregulate either PKC- α or PKC- ζ (**Fig. 3f,g**) providing further evidence that ES-62 signals through a distinct TLR4 mechanism.

To demonstrate the activity of ES-62 against mast cells *in vivo*, we used a mouse model of immediate-type hypersensitivity to oxazolone²². As indicated by knockout mouse studies, the immediate hypersensitivity response in this model is crucially dependent on functional mast cells²². Mast cells obtained from the ears of sensitized and challenged mice degranulated in response to Fc ϵ RI cross-linking *ex vivo*, but this degranulation was considerably reduced if animals had been inoculated with an amount of ES-62 appropriate to natural filarial nematode infection^{6,23} (**Fig. 4a**). Inhibition of degranulation correlated with lack of production of TNF- α (**Fig. 4b**), IL-3 and IL-6 (but not IL-5 and IL-13, **Supplementary Fig. 4** online) and suppression of NF- κ B activation (**Fig. 4c**) in response to Fc ϵ RI cross-linking *ex vivo*. Notably, ES-62 also inhibited the mast cell–dependent hypersensitivity reaction *in vivo*, as determined by measurement of ear swelling (**Fig. 4d**).

To demonstrate that ES-62 is active at other sites of mast cell–mediated inflammation, we tested its ability to inhibit degranulation in the lungs of mice sensitized to and challenged with ovalbumin.

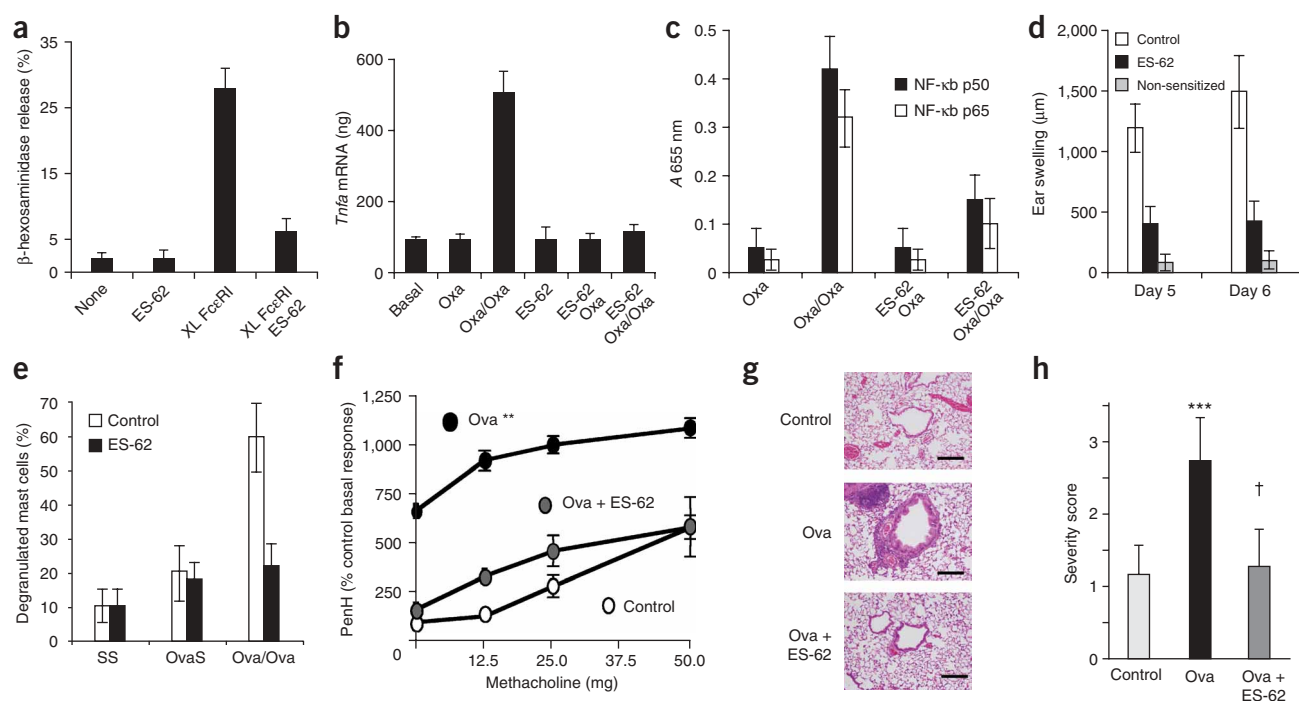


Figure 4 *In vivo* exposure to ES-62 inhibits mouse mast-cell activity *ex vivo* and protects against immediate hypersensitivity. **(a)** β -hexosaminidase release from mast cells from control and ES-62-treated mice sensitized and challenged on day 5 with oxazolone was determined after incubation with media (None and ES-62) or cross-linking of Fc ϵ RI for 30 min (XLFc ϵ RI and XLFc ϵ RI ES-62). Results shown are the means \pm s.d., $n = 3$ and are representative of two separate experiments. **(b)** Mast cells were isolated from control and ES-62-treated mice before sensitization with oxazolone (Basal), after sensitization (Oxa) and after challenge (Oxa/Oxa). Total RNA was extracted and *Tnfa* mRNA levels were measured by RT-PCR. **(c)** NF- κ B p50 and p65 activity in nuclear extracts from purified mast cells from control and ES-62-treated oxazolone-sensitized mice who were either non-challenged controls (Oxa) or oxazolone challenged (Oxa/Oxa). **(d)** Control (Control) and ES-62-treated (ES-62) mice were sensitized with oxazolone and challenged on days 5 and 6. Nonsensitized mice were also challenged (non-sensitized). Ear swelling was measured 1 h after challenge. For **b**, **c** and **d**, all values represent the means \pm s.d., comprising pooled data from three independent experiments. **(e)** Control and ES-62-treated mice were sensitized and challenged with ovalbumin (Ova/Ova), sensitized with ovalbumin and challenged with saline (OvaS) or sensitized and challenged with saline (SS). Intact and degranulating mast-cell counts in lung tissue were determined, and the data are expressed as the percentage degranulated mast cells (mean \pm s.d. values for three independent experiments). **(f–h)** ES-62- or saline-treated mice were sensitized and challenged with ovalbumin, and non-sensitized mice (control) received ES-62 alone. **(f)** Methacholine responses were examined 24 h after the last challenge. Results are expressed as means \pm s.d., $^{**}P < 0.01$ for Ova versus control or versus Ova + ES-62. **(g)** Mice were killed on day 28 and bronchoalveolar lavage was performed. Sections of lung tissue from control mice (top), Ova-sensitized and challenged mice (middle) and Ova sensitized and challenged mice treated with ES-62 (bottom) were stained by H&E. Scale bar represents 250 μ m. **(h)** Lung infiltrate was scored blindly for peribronchial cuffing, mucosal hyperplasia and infiltrates of lymphocytes and eosinophils, on a scale of 1 = normal, 2 = mild, 3 = moderate and 4 = severe in 100 random bronchiole walls. Data are expressed as means \pm s.d. $^{***}P < 0.001$ Ova versus control; $^{\dagger}P < 0.001$ Ova + ES-62 versus Ova using the Mann-Whitney *U*-test comparing group medians.

ES-62 was clearly active in these experiments (**Fig. 4e** and **Supplementary Fig. 5** online). This again highlights the differences between ES-62- and LPS-mediated TLR4 signaling, as it has been shown that LPS increases mast cell-dependent airway inflammation²⁴. Also, mast cells, but not T cells or eosinophils, localize within bronchial smooth muscle in individuals with asthma, where mast cell mediators promote tissue remodeling leading to hyperreactive lung function²⁵. We therefore assessed whether ES-62 could prevent airway remodeling and hence disease progression. To this end, we used unrestrained barometric plethysmography to quantify changes in lung function in response to the bronchoconstricting agent methacholine²⁶. ES-62 clearly suppressed such airway hyperresponsiveness (**Fig. 4f**). Moreover, we also found that disease severity and progression are reduced by ES-62 in this model, as measured by each of the accepted parameters of histological analysis of lung pathology (**Fig. 4g,h**), lung eosinophilia and the release of the signature cytokine necessary for the development of airway inflammation, IL-4 (**Supplementary Fig. 5** online). However, the degree to which this reflects direct

targeting of mast cells as opposed to other immune system components remains to be established.

Suppression of mast-cell function by ES-62 offers a new explanation for the reason why people harboring worms of at least the filarial nematode type show reduced incidence of allergy, in spite of their elevated serum IgE. Certainly, the majority of studies undertaken indicate that the absence of allergy in developing countries is not due to a lack of allergen sensitization but to a loss of immune effector functions³. By inhibiting mast-cell effector function, ES-62 offers a new potential therapeutic approach for diseases such as asthma, a medical problem of enormous importance in the developed world. Although ES-62 *per se* is unlikely to be used for treatment, enough is known about its structure and function²⁷ to allow one to envisage the development of small, presumably phosphorylcholine-based, derivatives as drugs. In relation to this, an important point to consider is that the parent molecule is well tolerated by the tens of millions of infected people in the tropics, often for their entire lives.

METHODS

ES-62. We prepared highly purified, endotoxin-free ES-62 from the rodent filarial nematode *Acanthocheilonema viteae*²⁸. This protein is ~77% homologous to the ES-62 of the human filarial nematode *Brugia malayi*²⁹ and contains the same nematode-specific post-translational modification of phosphorylcholine linked to N-type glycans⁴.

FcεRI aggregation. We collected bone marrow from healthy volunteers who provided formal consent according to the protocol approved by the US Food and Drug Administration Committee for Research Involving Human Subjects. Bone marrow-derived mast cells (BMMCs) were generated as previously described (>95% CD45⁺CD117⁺CD9⁺FITC-IgE⁺chymase⁺CD4⁺CD8⁺CD11b⁺CD11c⁺MHCII⁺)⁷. We sensitized BMMCs with 1 μg/ml human 2,4-dinitrophenol (DNP)-specific IgE for 18 h in the presence or absence of 2 μg/ml ES-62 or 500 ng/ml LPS. BMMCs were activated by the antigen DNP-human serum albumin (HSA) (1 μg/ml) for the times indicated.

β-hexosaminidase release. We assessed degranulation of β-hexosaminidase⁷ by incubating sample supernatants with 200 μl of 1 mM *p*-nitrophenyl *N*-acetyl-β-D-glucosaminide for 1 h at 37 °C before measuring the optical density at 405 nm. Total β-hexosaminidase was determined by extraction with 1% Triton X-100.

Cytosolic calcium. We loaded sensitized cells with 1 μg/ml Fura2-AM (Molecular Probes) in PBS, 1.5 mM Ca²⁺ and 1% BSA. FcεRI was aggregated and fluorescence was measured⁷.

Signaling assays. We measured PLD activity after BMMC labeling (10⁶ cells/ml) with [³H]palmitic acid (5 μCi/ml, Amersham) for the 18-h sensitization period. FcεRI was aggregated in the presence of butan-1-ol (0.3% final concentration) and the resultant [³H]phosphatidylbutanol was assayed⁷. We measured SPHK activity by the transfer of the γ-phosphate group of [γ-³²P]ATP (1 μCi/sample) to sphingosine, separating the products by thin-layer chromatography on silica gel G60 (Whatman)⁷. We measured PKC enzyme activity by the transfer of the γ-phosphate group of [γ-³²P]ATP (1 μCi/sample) to a peptide substrate specific for PKC (Protein Kinase C Biotrak assay system, Amersham)⁸.

Western blotting analysis of PKC isoforms. We probed cell lysates (40 μg; quantified using the Bradford reagent system (Bio-Rad)) with antibodies to PKC-α, PKC-β, PKC-γ, PKC-δ, PKC-ε, PKC-ι (BD Biosciences) and PKC-ζ (Santa Cruz) and visualized the blots with an antibody to mouse Ig conjugated to horseradish peroxidase (Amersham Biosciences) and the enhanced chemiluminescence Western Blotting Detection System (GE Healthcare). In some experiments, cells were pretreated with nystatin (50 μg/ml; Calbiochem) or lactacystin (25 μM; Biomol) for 30 min and then cultured with ES-62 or in ES-62-free medium overnight at 37 °C before preparation of extracts for western blotting.

Antisense treatment of mast cells. We incubated differentiated mast cells, 1.5 × 10⁶/ml, with or without 10 μM phosphorothioate-protected antisense oligonucleotides with oligofectamine (Invitrogen) for 48 h before FcεRI cross-linking^{7,8}. Details of the oligonucleotides are provided in **Supplementary Methods** online.

Eicosanoid and cytokine detection. We evaluated levels in culture supernatants by ELISA (R&D Systems and Cayman Chemicals).

NF-κB activity. We analyzed NF-κB activity by using the BD Mercury TransFactor Profiling Kit—Inflammation. We demonstrated the specificity of the p50 and p65 interactions with nuclear cell extracts by using increasing amounts of competitor oligonucleotides.

Confocal microscopy. We incubated cells with FITC-conjugated ES-62 (made in-house) at 4 °C for 30 min. Cells were then washed and incubated at 37 °C for the times specified before they were fixed with 1% paraformaldehyde for 10 min at room temperature, transferred onto glass slides with a cyto-spin and permeabilized with 0.5% Triton X-100. We visualized TLR4 expression by staining with a monoclonal TLR4-specific antibody (BD Biosciences) followed

by rabbit antibody to mouse Ig conjugated to tetramethylrhodamine isothiocyanate (Invitrogen) and subsequently analyzed the cells on a Zeiss LSM510 confocal microscope.

Western blot analysis of TLR4- and ES-62-containing immune complexes. We incubated mast cells with LPS (500 ng/ml per 3 × 10⁶ cells/ml) or FITC-conjugated ES-62 at 4 °C for 30 min. After this, the cells were washed and incubated at 37 °C and incubations were stopped by lysis in digitonin-containing buffer at the times specified. Cell lysates and, in some experiments, the antigen-depleted cell lysates were incubated with antibodies and western blotting was carried out as described in **Supplementary Methods**.

Oxazolone skin sensitization model of immediate-type hypersensitivity. Full details of this procedure are in **Supplementary Methods**.

Real-time quantitative PCR. We extracted RNA using the Trizole method (Invitrogen) and further purified it using RNeasy columns (Qiagen). Real-time PCR was performed with the LightCycler RNA Master SYBR Green Kit (Roche) in a LightCycler instrument (Roche) using primers specific for cytokine genes, the details of which are in **Supplementary Methods**.

Ovalbumin airway hypersensitivity model. We sensitized female 8-week-old BALB/c mice by intraperitoneally injecting 100 μg ovalbumin (Ova)/4 mg Al(OH)₃ on days 0 and 14. On days 14, 25, 26 and 27, the animals were challenged with intranasal application of 10 μg Ova in 30 μl of saline under avertin anesthesia. We injected ES-62 (2 μg/animal) or saline (control) subcutaneously on days 2, 12, 25 and 27. Full details of assessment of mast-cell degranulation, measurement of airway hyperreactivity to methacholine, bronchoalveolar lavage analysis and assessment of lung histology are in **Supplementary Methods**.

Additional methods. Detailed methodology is described in **Supplementary Methods**.

Note: Supplementary information is available on the Nature Medicine website.

ACKNOWLEDGMENTS

This work was supported by grants from the Yong Loo Lin School of Medicine, the National University of Singapore (A.J.M.) and the Wellcome Trust (W.H. and M.M.H.).

Published online at <http://www.nature.com/naturemedicine>

Reprints and permissions information is available online at <http://npg.nature.com/reprintsandpermissions>

1. Burney, P.G.J. Epidemiological trends. In *Asthma* (eds. Barnes, P.J., Grunstein, M.M., Leff, A.R. & Woolcock, A.J.) 35–47 (Lippincott Raven, Philadelphia, 1997).
2. McKay, D.M. The beneficial helminth parasite? *Parasitology* **132**, 1–12 (2006).
3. Wilson, M.S. & Maizels, R.M. Regulation of allergy and autoimmunity in helminth infection. *Clin. Rev. Allergy Immunol.* **26**, 35–50 (2004).
4. Harnett, W., McInnes, I.B. & Harnett, M.M. ES-62, a filarial nematode-derived immunomodulator with anti-inflammatory potential. *Immunol. Lett.* **94**, 27–33 (2004).
5. Kinet, J.P. The high-affinity IgE receptor (FcεRI): from physiology to pathology. *Annu. Rev. Immunol.* **17**, 931–972 (1999).
6. Lal, R.B., Paranjape, R.S., Briles, D.E., Nutman, T.B. & Ottesen, E.A. Circulating parasite antigen(s) in lymphatic filariasis—use of monoclonal-antibodies to phosphocholine for immunodiagnosis. *J. Immunol.* **138**, 3454–3460 (1987).
7. Melendez, A.J. & Khaw, A.K. Dichotomy of Ca²⁺ signals triggered by different phospholipid pathways in antigen stimulation of human mast cells. *J. Biol. Chem.* **277**, 17255–17262 (2002).
8. Melendez, A.J., Harnett, M.M. & Allen, J.M. Crosstalk between ARF6 and protein kinase Calpha in FcγRI-mediated activation of phospholipase D1. *Curr. Biol.* **11**, 869–874 (2001).
9. Li, G., Lucas, J.J. & Gelfand, E.W. Protein kinase Cα, βI and βII isozymes regulate cytokine production in mast cells through MEK2/ERK5-dependent and independent pathways. *Cell. Immunol.* **238**, 10–18 (2005).
10. Abdel-Raheem, I.T. *et al.* Protein kinase C-α mediates TNF release process in RBL-2H3 mast cells. *Br. J. Pharmacol.* **145**, 415–423 (2005).
11. Coward, W.R. *et al.* NF-κB and TNF-α: a positive autocrine loop in human lung mast cells? *J. Immunol.* **169**, 5287–5293 (2002).
12. Stassen, M. *et al.* IL-9 and IL-13 production by activated mast cells is strongly enhanced in the presence of lipopolysaccharide: NF-κB is decisively involved in the expression of IL-9. *J. Immunol.* **166**, 4391–4398 (2001).
13. Jeong, H.J. *et al.* Role of Ca²⁺ on TNF-α and IL-6 secretion from RBL-2H3 mast cells. *Cell. Signal.* **14**, 633–639 (2002).

14. Marquardt, D.L. & Walker, L.L. Dependence of mast cell IgE-mediated cytokine production on nuclear factor- κ B activity. *J. Allergy Clin. Immunol.* **105**, 500–505 (2000).
15. Dolmetsch, R.E., Xu, K. & Lewis, R.S. Calcium oscillations increase the efficiency and specificity of gene expression. *Nature* **392**, 933–936 (1998).
16. Goodridge, H.S. *et al.* Immunomodulation via novel use of TLR4 by the filarial nematode phosphorylcholine-containing secreted product, ES-62. *J. Immunol.* **174**, 284–293 (2005).
17. Rhee, S.H. & Hwang, D. Murine Toll-like receptor 4 confers lipopolysaccharide responsiveness as determined by activation of NF κ B and expression of the inducible cyclooxygenase. *J. Biol. Chem.* **275**, 34035–34040 (2000).
18. Powner, D.J., Hodgkin, M.N. & Wakelam, M.J. Antigen-stimulated activation of phospholipase D1b by Rac1, ARF6, and PKC α in RBL-2H3 cells. *Mol. Biol. Cell* **13**, 1252–1262 (2002).
19. Leontieva, O.V. & Black, J.D. Identification of two distinct pathways of protein kinase C α down-regulation in intestinal epithelial cells. *J. Biol. Chem.* **279**, 5788–5801 (2004).
20. Li, L., Cousart, S., Hu, J. & McCall, C.E. Characterization of interleukin-1 receptor-associated kinase in normal and endotoxin-tolerant cells. *J. Biol. Chem.* **275**, 23340–23345 (2000).
21. Smith, L. *et al.* Activation of atypical protein kinase C ζ by caspase processing and degradation by the ubiquitin-proteasome system. *J. Biol. Chem.* **275**, 40620–40627 (2000).
22. Bryce, P.J. *et al.* Immune sensitization in the skin is enhanced by antigen-independent effects of IgE. *Immunity* **20**, 381–392 (2004).
23. Goodridge, H.S. *et al.* Modulation of macrophage cytokine production by ES-62, a secreted product of the filarial nematode. *Acanthocheilonema viteae*. *J. Immunol.* **167**, 940–945 (2001).
24. Nigo, Y.I. *et al.* Regulation of allergic airway inflammation through Toll-like receptor 4-mediated modification of mast cell function. *Proc. Natl. Acad. Sci. USA* **103**, 2286–2291 (2006).
25. Bradding, P., Walls, A.F. & Holgate, S.T. The role of the mast cell in the pathophysiology of asthma. *J. Allergy Clin. Immunol.* **117**, 1277–1284 (2006).
26. Hamelmann, E. *et al.* Noninvasive measurement of airway responsiveness in allergic mice using barometric plethysmography. *Am. J. Respir. Crit. Care Med.* **156**, 766–775 (1997).
27. Harnett, W., Harnett, M.M. & Byron, O. Structural/functional aspects of ES-62—a secreted immunomodulatory phosphorylcholine-containing filarial nematode glycoprotein. *Curr. Protein Pept. Sci.* **4**, 59–71 (2003).
28. McInnes, I.B. *et al.* A novel therapeutic approach targeting articular inflammation using the filarial nematode-derived phosphorylcholine-containing glycoprotein ES-62. *J. Immunol.* **171**, 2127–2133 (2003).
29. Goodridge, H.S., Stepek, G., Harnett, W. & Harnett, M.M. Signalling mechanisms underlying subversion of the immune response by the filarial nematode secreted product ES-62. *Immunology* **115**, 296–304 (2005).